Basic studies of the generation and collective motion of pair-ion plasmas[a)]

W. Oohara[b)] and R. Hatakeyama[c)]
Department of Electronic Engineering, Tohoku University, Sendai 980-8579, Japan

(Received 29 October 2006; accepted 4 January 2007; published online 22 March 2007)

A fullerene pair-ion plasma without electrons is generated and electrostatic modes propagating along magnetic-field lines are externally excited in the range of low frequencies. It is found that four kinds of wave modes, including theoretically unexpected ones, exist in the plasma, and the phase lag between the density fluctuations of positive and negative ions strongly depends on the frequency. In order to illuminate further collective motion of pair-ion plasmas in the range of high frequencies, a concept of a hydrogen pair-ion plasma consisting of only H^+ and H^- is proposed and an experimental configuration is presented. On the basis of the production of a hydrogen plasma by Penning ionization gauge discharge, the principles of ion cyclotron resonance and $E\times B$ drift motion are shown to be effective for ion-species analysis/selection and separated electron detection from negative ions in the generation of pure hydrogen pair-ion plasmas. © *2007 American Institute of Physics*. [DOI: 10.1063/1.2436854]

I. INTRODUCTION

Pair plasmas consisting of only positive- and negative-charged particles of equal mass have attracted special attention. Such pair plasmas maintain space-time symmetry because the mobility of the particles in electromagnetic fields is the same. Positrons have been spotlighted in connection with antimatter properties, e.g., CPT [charge conjugation (C), parity inversion (P), and time reversal (T)] invariance, in high-energy physics and astrophysics, and pair plasmas consisting of positrons and electrons have been investigated theoretically.[1–7] Both the relativistic and nonrelativistic pair plasmas have been gradually revealed to represent a new state of matter with unique thermodynamic properties drastically different from those of ordinary electron-ion plasmas. Some theoretical works have already been presented, which concern the elementary properties and the linear and nonlinear collective modes in nonrelativistic electron-positron plasmas. A comprehensive two-fluid model has been developed for collective-mode analyses, based on which longitudinal/transverse-electrostatic/electromagnetic modes have been studied, and the experimental identification is desired to be undertaken at present. Plasmas including positrons have been generated experimentally in laboratories.[8–13] In particular, the electron-positron plasma is experimentally generated by injecting a low-energy electron beam into a positron plasma. For long-time-scale plasma physics experiments, it is necessary to meet the condition that the annihilation time scale is many orders of magnitude larger than the plasma period. In order to maintain a steady-state plasma over such long durations the pairs must be created prolifically to balance their short annihilation time scales. Thus, it is not easy to generate and maintain the electron-positron plasma. Here, our attention is concentrated on the easy and stable-state generation of a pair-ion plasma consisting of positive and negative ions of equal mass, and its collective-mode identification.

According to our previous work on the generation of an alkali-fullerene plasma (K^+, e^-, C_{60}^-) by introducing a fullerene into a potassium plasma,[14–17] fullerenes are candidates for the ion source to realize the pair-ion plasma, because the interaction of electrons with the fullerenes leads to the production of both negative and positive ions. We have developed a novel method of generating a pair-ion plasma that consists of only positive and negative ions of equal mass, using fullerene.[18–21] Since the frequency range of interesting collective phenomena is limited to low frequencies in this case of fullerene pair-ion plasmas due to massive ions, an attempt is made to generate hydrogen pair-ion plasmas consisting of the light H^+ and H^- ions, which are suitable for studying novel collective phenomena in the range of high frequencies. Here we report the basic studies of the generation and collective motion of the fullerene and hydrogen pair-ion plasmas.

II. FULLERENE PAIR-ION PLASMA GENERATION

A pair-ion plasma source with fullerene ion species consists of an electron-beam gun, an ion production cylinder, and a magnetic filter.[18–21] The electron-beam gun is set inside the ion production cylinder (8 cm diam and 30 cm length) with a thin annulus (inner diameter 3 cm and 0.1 cm thickness) made of copper. The plasma source is installed in a grounded vacuum chamber of 15.7 cm diam and 260 cm length, as shown schematically in Fig. 1. A uniform magnetic field of $B=0.2$ T is applied using solenoid coils, and the background gas pressure is 2×10^{-4} Pa. A tungsten wire cathode with a ring structure of 5 cm diam is divided into four parts, which are connected in parallel, and which is resistively heated to over 2000 °C. The wire cathode is biased at voltage $V_k(<0$ V) with respect to a grounded grid anode set at less than 0.5 cm in front of the cathode. A stainless-steel disk of 4 cm diam is concentrically welded onto the grid anode. Thermally emitted low-energy electrons (~0.2 eV) are accelerated by the electric field between the

[a)]Paper QI2, 3, Bull. Am. Phys. Soc. **51**, 222 (2006).
[b)]Electronic mail: oohara@ecei.tohoku.ac.jp
[c)]Invited speaker. Electronic mail: hatake@ecei.tohoku.ac.jp

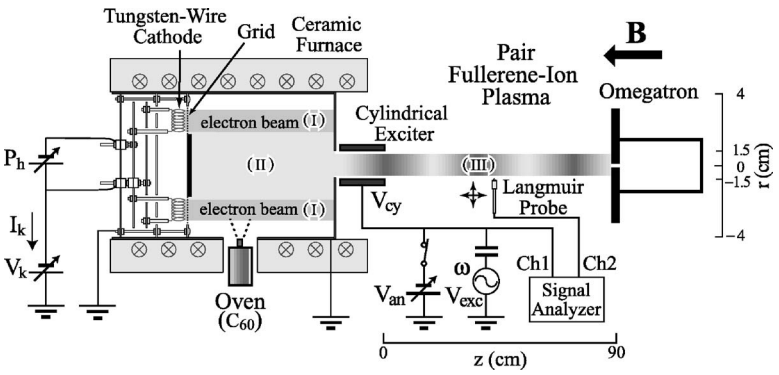

FIG. 1. Schematic drawing of fullerene pair-ion plasma source and measurement circuit. Longitudinal-electrostatic wave modes propagating along *B*-field lines are excited by a cylindrical exciter. Region (I) is the hollow electron-beam part, region (II) is the magnetic filtering part, and region (III) is the experimental part.

cathode and the anode, and form a hollow electron beam. The cylinder and the annulus are grounded, and the beam flows along the magnetic (B)-field lines and is terminated at the annulus. The beam energy E_e can be controlled in the range of 0–150 eV by changing V_k. The cylinder has a hole (3 cm diam) on the sidewall at which an oven for fullerene sublimation is set. A fullerene sample, which is commercially available C_{60} powder of 99.5% purity, is heated in the oven. Typical oven temperatures under operating conditions range between 400 and 600 °C. The fullerene vapor produced as a result of sublimation is made to fill the cylinder. The electron beam with an annular cross section collides with neutral C_{60}, and C_{60}^+ is produced by impact ionization.[22,23] Then low-energy electrons are simultaneously produced and they contribute to producing negative ions. Negative ions produced by electron attachment are singly charged,[24,25] and the process is simple compared with impact ionization. To produce C_{60}^+ and C_{60}^- concurrently, it is essential that C_{60} has the feature of electron attachment over a broad-energy range.

The chamber wall is grounded and an end plate is maintained at a floating potential. For analytic convenience, the whole space of the plasma is divided into three regions: (I), (II), and (III). The hollow electron-beam region is the fullerene-ion production region and is called region (I). Since charged-particle gyroradii are proportional to the $\sqrt{\text{mass/charge}}$ ratio, the gyroradius ratio $\rho_{C_{60}^\pm}/\rho_{e^-}$ is particularly high ($\simeq$1100). A preferential ambipolar diffusion of $C_{60}^\pm$ can take place in the radial (r) direction across the B-field lines due to their large gyroradii, i.e., a magnetic-filtering effect.[26] Only C_{60}^+ and C_{60}^- are expected to exist in the center of the cylinder, region (II), and the electron-free pair-ion plasma generation occurs here. C_{60}^+ and C_{60}^- flow along the B-field lines and pass through the annular hole toward the experimental region, region (III).

III. ELECTROSTATIC COLLECTIVE MODES IN FULLERENE PAIR-ION PLASMA

A cylindrical electrode is set in front of the annular hole between regions (II) and (III). The electrode can be biased at V_{an} superimposed by V_{exc} ($V_{cy}=V_{an}+V_{exc}$), where V_{an} is a dc voltage and V_{exc} is an ac voltage of frequency $\omega/2\pi$. The exit position of the electrode is defined as $z=0$ cm, and the pair-ion plasma is terminated at the end plate ($z=90$ cm). Plasma parameters in region (III) are measured using Langmuir probes, the collectors of which are surrounded with an insulator of ceramic and thus guarded against direct exposure to C_{60} particles and prevented from being contaminated by C_{60}. The generation property of the pair-ion plasma relative to the electron-beam energy E_e is measured. When E_e increases from 0 eV, the pair-ion plasma begins to be generated. The plasma density gradually increases and almost saturates at around $E_e=150$ eV. The plasma and floating potentials measured with the Langmuir probe are close to 0 V, which is almost equal to the potential of the grid and the annulus. The static potential structures including sheaths are found not to be formed in the pair-ion plasma because the mobilities of the ions are almost the same. The plasma density and the ion temperatures are calculated from the probe characteristics. The density is $1-2\times10^8$ cm^{-3} at $E_e=100$ eV, while the temperatures of C_{60}^+ and C_{60}^-, T_+ and T_-, are 0.3–0.5 eV. The plasma density can be modulated by temporally changing V_{cy}, enabling us to excite longitudinal-electrostatic modes in region (III) for $V_{exc}\neq0$. In the present situation it is extremely difficult to excite electromagnetic modes relevant to the plasma because the density and the temperature are relatively low and the induction current of the ions is very low.

Longitudinal-electrostatic modes are excited in region (III) by the cylindrical exciter.[18–20] The damping of the excited modes as they propagate depends on the frequency. V_{exc} must be small in the low-frequency range and large in the high-frequency range in order to maintain constant mode amplitude in the plasma for a variety of frequencies. The properties of mode propagation along the B-field lines are measured at $r=0$ cm, $z=4$–6 cm, and $E_e=100$ eV. The phase delay between the excited signal at frequency $\omega/2\pi$ and the fluctuation signal detected by the Langmuir probe is measured at each $z=4$, 5, and 6 cm, and the wave number k (wavelength) of the propagating modes is obtained from the average phase delay. $\omega/2\pi$ is changed from 0.1 to 50 kHz. The dispersion relation of the propagating modes is shown by closed circles in Fig. 2, where solid curves (mentioned below) are the calculated dispersion curves and the dashed line indicates the ion cyclotron frequency $\omega_c/2\pi=4.3$ kHz at $B=0.2$ T. For comparison, the previous results[19,21] are also shown as open circles. There are three modes in the measured dispersion relations, $\omega/2\pi<12$ kHz, $12<\omega/2\pi<20$ kHz, and $\omega/2\pi>20$ kHz, which we refer to as an ion acoustic wave (IAW), an intermediate-frequency wave

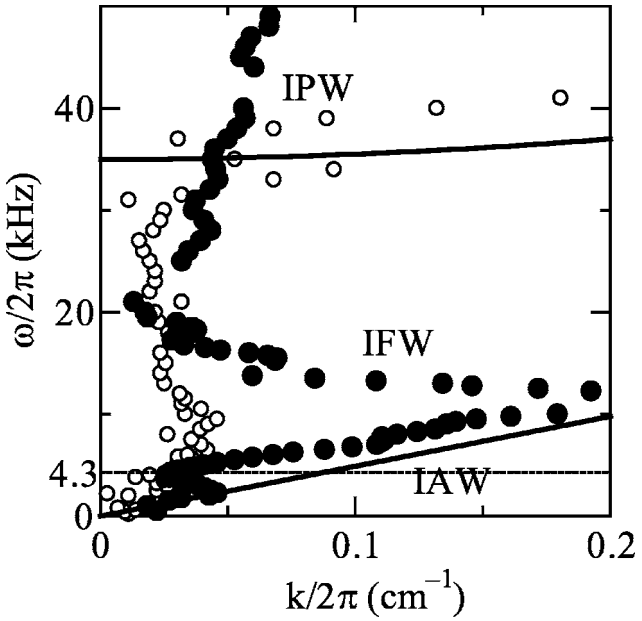

FIG. 2. Dispersion relations of electrostatic modes propagating along B-field lines. Closed circles indicate the dispersion relations measured at $r=0$ cm, $z=4-6$ cm, $E_e=100$ eV, and $B=0.2$ T. Solid curves are the calculated dispersion curves. The ion cyclotron frequency of C_{60} ions is 4.3 kHz, as indicated by the dashed line. For comparison, the previous results are also shown by open circles.

(IFW), and an ion plasma wave (IPW), respectively. IFW has the feature that the group velocity is negative but the phase velocity is positive, i.e., the mode resembles a backward wave. IAW can be measured in a larger $k/2\pi$ (shorter wavelength) range and IFW is measured more clearly, compared with the previous results,[19,21] because the structure of the exciter is improved and the amplitude of V_{cy} is adjusted in accordance with the variation of $\omega/2\pi$. Furthermore, it is definitely shown that IAW divides into two branches at around the ion cyclotron frequency $\omega_c/2\pi=4.3$ kHz. The measured dispersion relation of IPW is considerably changed compared with the previous result, the reason for which is not understood at present. The dispersion relations are linearized about a homogeneous unbounded plasma (ion temperatures $T=T_+=T_-$), and are simply given by

$$\omega^2 = c_s^2 k^2 \quad (\varphi = 0), \tag{1}$$

$$\omega^2 = c_s^2 k^2 + 2\omega_p^2 \quad (\varphi = \pi), \tag{2}$$

where the acoustic speed $c_s^2=\gamma T/m$ and the plasma frequency $\omega_p^2=e^2 n_0/\varepsilon_0 m$ are introduced (γ: ratio of specific heats C_p/C_v; n_0: plasma density). The phase lag φ between the oscillating components $\tilde{n}_+$ and $\tilde{n}_-$ of the positive and negative ion densities is defined as $\tilde{n}_+=\tilde{n}_-\exp(i\varphi)$. The dispersion relations (1) and (2) give modes that correspond to an acoustic wave and a plasma wave in ordinary plasmas, respectively. The dispersion relation corresponding to IFW cannot be derived in the simple two-fluid model. The dispersion curves described by Eqs. (1) and (2) have already been shown in Fig. 2, and were calculated for $\gamma=3$ [$\gamma=(2+N)/N$, one-dimensional compression $N=1$], $T=0.5$ eV (isotropy), and $n_0=1\times10^7$ cm^{-3}.

Temporal variations of $\tilde{n}_+$ and $\tilde{n}_-$ are measured and compared. The phase lag φ drastically changes depending on $\omega/2\pi$, which is not shown here. The phase lags of IFW and IPW in $\omega/2\pi>15$ kHz are π independent of frequency. The backward-like mode that connects the two divided branches is apparently analogous to IFW joining IAW and IPW, but the frequency dependence of the phase lag is quite different between this backward-like mode and IFW; that is, the backward-like mode has a strong frequency dependence of the phase lag, but IFW does not. The dependence cannot be derived in this theoretical formulation. Concerning the IPW property, IPW measured in the previous experiment, which is indicated by open circles in Fig. 2 (Refs. 19 and 21), fits relatively well to the calculated curve, but IPW considerably differs from the calculated one here. The phase lag of IPW is $\varphi=\pi$, as theoretically expected from Eq. (2), and IPW does not have the frequency dependence. The phase lags of IFW and IPW reverse, which means that a charge separation is realized and electrostatic-potential structures are formed in the pair-ion plasma in the dynamical state. This phenomenon is in contrast to the measured result that the electrostatic-potential structures including sheaths are almost not formed in the stationary state. In ordinary electron-ion plasmas, φ is close to zero for IAW. On the other hand, φ is not defined for an electron plasma wave (synonymous with IPW in the pair-ion plasma) because the ion response is very slow compared with that of electrons, and the ion-density fluctuation is ignored. Thus, IPW with $\varphi\simeq\pi$ reflects a special situation and, accordingly, IFW is found to display a unique property, which is exemplified by the backward-like mode and the phase inversion of the density fluctuations. No interference or correlation between IAW and IPW appears in ordinary plasmas because the frequency bands of IAW and IPW are widely different. In the case of the pair-ion plasma, the frequency band of IPW becomes close to that of IAW and is accompanied by the appearance of IFW. This situation is the same as the backward-like mode in $2.5<\omega/2\pi<4.3$ kHz. Thus, these backward-like modes are considered to be caused by the transition from one mode to another, with a similar frequency. Such a dispersion property is one of the unique phenomena of the pair-ion plasma, while these backward-like modes do not appear in ordinary electron-ion plasmas. Not only the properties of linear electrostatic waves but also those of nonlinear waves and electromagnetic waves in relation to the present pair-ion plasmas have been investigated theoretically,[27–42] but their theoretical identification has not been achieved at present.

IV. HYDROGEN PAIR-ION PLASMA GENERATION

The response frequency of the fullerene pair-ion plasma is limited to the narrow frequency range below 50 kHz. In order to expand the domain of the physical-properties elucidation of pair-ion plasmas and to investigate the wave-propagation characteristic up to high frequencies (MHz order), the development of a new pair-ion plasma source has been started. Since hydrogen is the most fundamental element of the periodic table, we here aim to generate a pair-ion plasma consisting of hydrogen ions (H^+-H^-) that have small

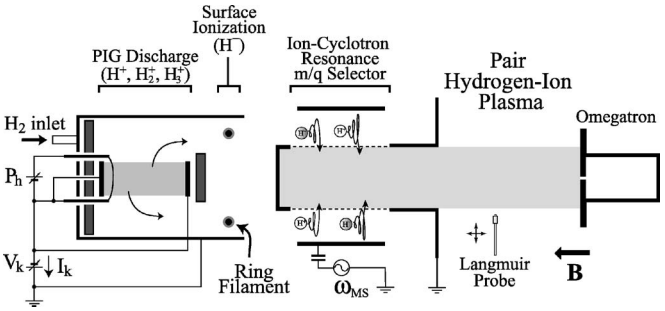

FIG. 3. Schematic drawing of hydrogen pair-ion plasma source. The plasma source consists of a PIG discharge part (H^+, H_2^+, H_3^+), a surface ionization part (H^-), and an ion selector. The omegatron is situated behind the end plate.

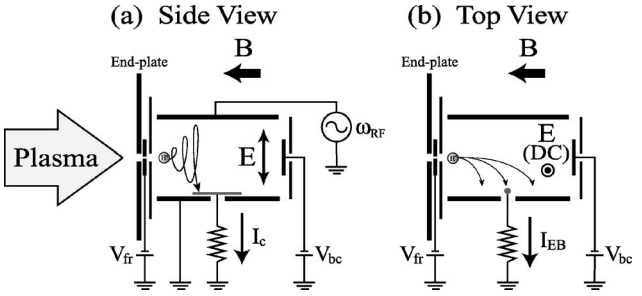

FIG. 4. Ion species in the plasma are analyzed using the omegatron. Schematic (a) side and (b) top views of the omegatron.

mass and high response frequency to electromagnetic fields. The equipment outline for the hydrogen pair-ion plasma generation and measurement is illustrated in Fig. 3. The plasma source comprises a Penning ionization gauge (PIG)-discharge part, a negative-ion production part, and an ion selection part. Two cathode disks are oppositely located on the center axis of the cylinder, similar to how an anode is located in a uniform B field, and a tungsten filament of 1 mm diam is set in front of one of the cathodes to supply thermal electrons. The thermal electrons are accelerated in a sheath formed in front of the cathode and injected into the space between the two cathodes, and the electrons are reflected in a sheath formed in front of the opposite cathode (anticathode) because the same voltage is applied to the two cathodes. Since the beam electrons are electrostatically confined between the two cathodes along the B-field lines, neutral molecules can be dissociated and ionized efficiently by electron impact. The electrons pass transversely across the B-field lines and reach the cylindrical anode, and thus a discharge current I_k is observed to flow. I_k differs from the discharge current in ordinary dc discharges of parallel cathode-anode plates, and the electron current in the plasma along the B-field lines is 10^2–10^3 times higher than I_k. Therefore, the ionization degree is relatively high and the plasma density can easily be increased. This discharge method is known as PIG discharge, and is also used for multicharged ion production. To separate the beam electrons and the bulk electrons from the ions, the hollow-cylinder diffusion plasma surrounding the core PIG plasma is utilized.

The energy range of electron attachment is about 1 eV for the production of negative hydrogen ions H^-, so the volume production of H^- in the gaseous phase is quite difficult compared with C_{60} ($\sim$10 eV). According to the research and development on neutral beam injection (NBI) heating for fusion-oriented plasmas, it has been found that the surface production of H^- is efficient on a warm Cs-coated plate with a low work function. Since there is the possibility of impurity incorporation into the hydrogen pair-ion plasma, however, alkali metals with low evaporation temperature cannot be used here. Instead, the production of negative ions is attempted on a heated ring filament coated with BaO (work function $>$1.5 eV) or LaB_6 ($>$2.7 eV), which is set between the negative-ion production and ion selection parts in the hollow-cylinder plasma. The plasma is here considered to consist of H^+, H_2^+, H_3^+, H^-, and electrons, and hence, H_2^+, H_3^+, and electrons must be removed to obtain the hydrogen pair-ion plasma. To separate the ions, we have adopted the principle of ion-cyclotron resonance with a double cylinder arrangement. The inner cylinder consists of a grounded rolled grid and the ions can further penetrate to the inner central space. When rf voltage is applied to the outer cylinder, a radial E field is formed between the cylinders, in the direction perpendicular to the B-field lines. When the rf frequency coincides with the cyclotron frequency of H^+ and H^-, their Larmor radii become large owing to the resonance, and they selectively diffuse to the inner central space, i.e., ion-species selection is accomplished.

Three important steps in hydrogen pair-ion plasma generation are positive-ion production, negative-ion production, and H^+/H^- selection. It is necessary to analyze correctly the ion species included in the plasma at each step. The cyclotron resonance phenomenon has been regarded as an attractive method of measuring the charge-to-mass ratio of ions ever since the development of the cyclotron. The omegatron is an rf mass spectrometer which has been used conventionally for mass determination.[43–47] In the omegatron, an rf electric field is set up normal to a uniform B field, and ions are excited at their various cyclotron resonances, causing their orbital radii to increase; the current induced when they strike a collector is measured. The omegatron with an $E\times B$ drift collector is schematically shown in Fig. 4; the role of dc $E\times B$ drift under the present configuration is described below. The omegatron is situated behind the end plate kept at a floating potential, which has a center hole of 5 mm diam, and its volume is about $5\times10\times10$ cm^3. The omegatron consists of an rf electrode (top plate, 10×10 cm^2), a ground electrode (bottom plate), a front electrode with an aperture of 0.5 mm diam, a back electrode, a collector grounded via a resistance, two side plates, and the $E\times B$ drift collector set on the side plate. The front electrode is made of copper of 1 mm thickness, to which a dc bias voltage V_{fr} in the range of $-60<V_{fr}<+10$ V is applied. V_{fr} has significant effects on the omegatron performance and charged-particle selection (described below). When V_{fr} is sufficiently lower than the plasma potential, only positive ions enter into the omegatron. Negative ions and electrons, on the other hand, can enter only when V_{fr} is sufficiently higher. The back electrode is biased in the range of $-5<V_{bc}<+5$ V, which retards the

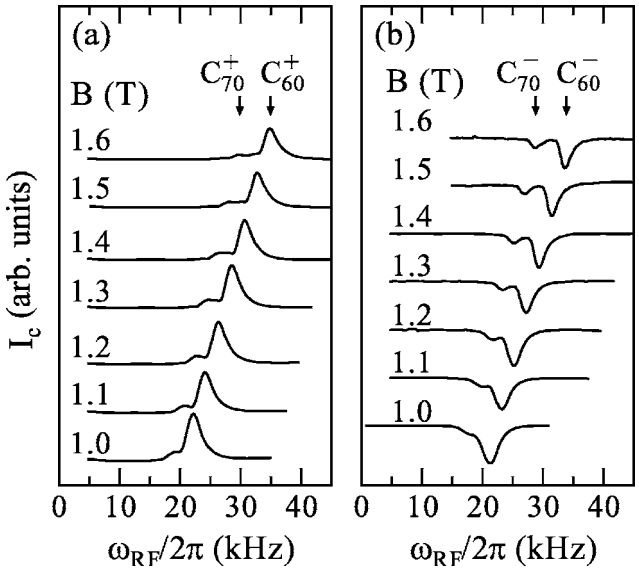

FIG. 5. Frequency spectra of the collector current I_c for various values of B field: (a) positive and (b) negative ions in the fullerene-ion plasma.

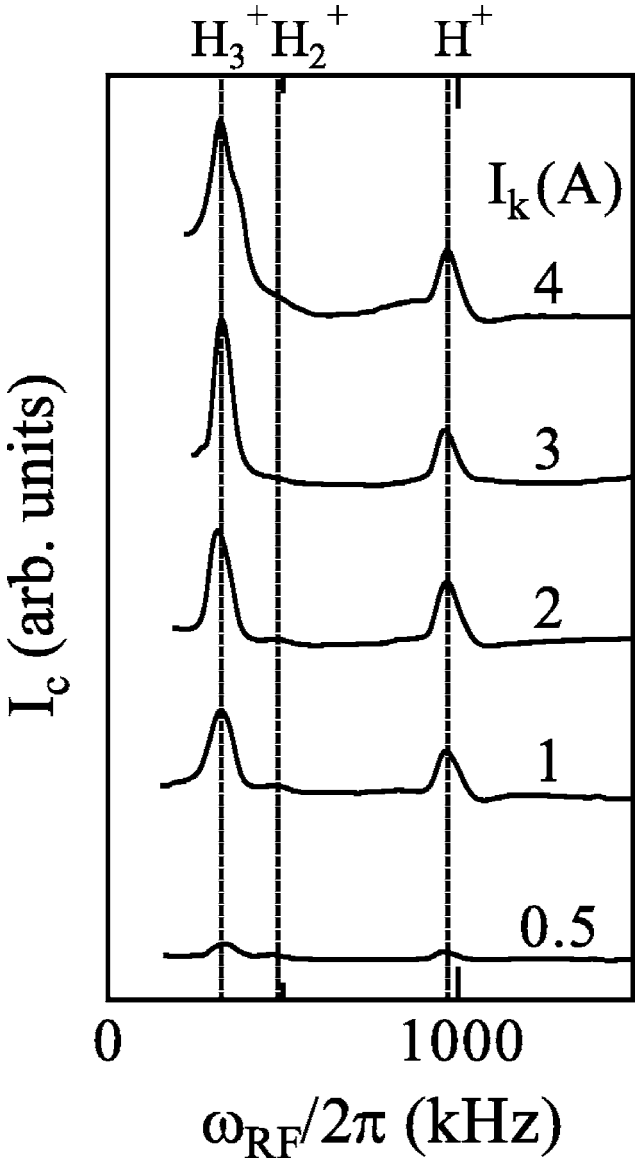

FIG. 6. Frequency spectra of I_c for various values of discharge current I_k at B=65 mT in the hydrogen-ion plasma.

charged particles along the B-field lines. The side plates are made of mica because insulator plates do not disturb electric fields formed between the top and the bottom plates. An rf E field that crosses a constant B field is formed in the 5-cm gap between the top and bottom plates. The spatial distribution of the rf field is essentially uniform throughout the working volume because of aspect-ratio control. The amplitude and the frequency of the rf field are 2 V/cm and less than 1.5 MHz, respectively. The ions entering from the aperture encounter the rf field. If the frequency of the rf field coincides with the ion cyclotron frequency ($\omega_c=qB/m$) for a particular species, the ions move considerably further away from the axis of the omegatron along a spiral trajectory than nonresonant ions. The resonant ions strike the collector situated off axis, thus providing an indication of resonance. The ions flow into the collector and a time-averaged ion current I_c is measured via a resistor of 1 MΩ. Thus, a spectrum of the ion current as a function of the rf frequency $\omega_{RF}/2\pi$ is obtained by slow sweep of the frequency. This measurement method is called the chirp method and is convenient, even though it has no advantage in mass resolution over the stored waveform inverse Fourier transform (SWIFT) method which is used in the Fourier transform ion cyclotron resonance (FT-ICR) mass spectrometer.

First, the ion species in the fullerene and hydrogen pair-ion plasmas are designed to be analyzed using the omegatron. In order to evaluate the mass resolution of the omegatron, a fullerene-ion plasma is generated in a similar way as that shown in Fig. 1, where not a pure fullerene but a mixture of C_{60} (70%) and C_{70} (30%) is used as a sample. Thus, the plasma includes C_{60}^+, C_{60}^-, C_{70}^+, and C_{70}^-. The B field is strengthened in the range of B=1–1.6 T for mass-resolution improvement. The frequency spectra of the collector current I_c are presented in Fig. 5, where the positive (a) and negative (b) currents of I_c indicate the currents of the positive ions (C_{60}^+,C_{70}^+) and the negative ions (C_{60}^-,C_{70}^-), respectively. The current peaks are shifted in proportion to the B-field strength, and the peaks of the massive C_{60} and C_{70} ions are found to be clearly separable.

Next, the hydrogen-ion species are analyzed using the omegatron at the step of positive-ion production in the PIG discharge, and hence the negative-ion production and H^+/H^- selection are not performed here. The H_2 gas pressure is 4×10^{-2} Pa, the discharge voltage V_k is fixed at around −300 V, and the plasma density is of the order of 10^{10} cm^{-3}. The frequency spectra of I_c for various values of discharge current I_k at B=65 mT are shown in Fig. 6. The ion cyclotron frequency of H^+ is calculated to be $\omega_c/2\pi$=995 kHz. The peaks at the one-half and the one-third frequencies of the H^+ resonance frequency indicate the existences of H_2^+ and H_3^+, respectively. The H_3^+ density is high in the plasma, but the H_2^+ density is very low. H_3^+ is produced by the process $H_2^+ + H_2 \rightarrow H_3^+ + H$, and H_2^+ is converted into H_3^+ as soon as it is produced.[48–50] Thus, the collision between H_2^+ and H_2 is considered to occur frequently in this situation. Figure 7 presents

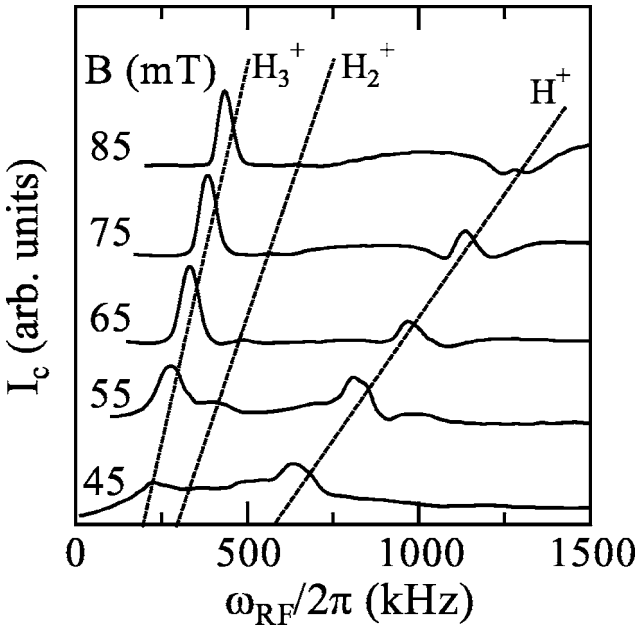

FIG. 7. Frequency spectra of I_c for various values of B field at I_k=2 A in the hydrogen-ion plasma.

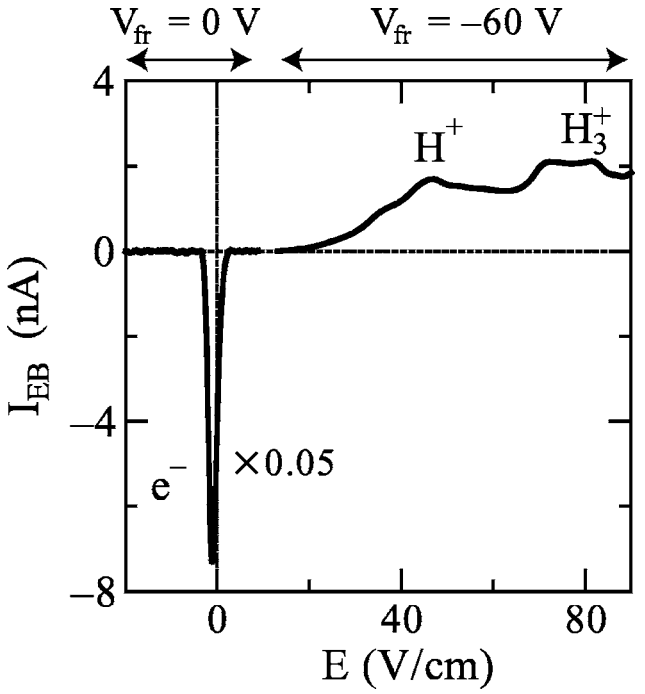

FIG. 8. Collector current I_{EB} relative to dc electric field. The collector is set on the side plate of the omegatron.

the frequency spectra of I_c for various values of the B field at I_k=2 A. The current peaks are shifted in proportion to the B field and the peaks of H^+ and H_3^+ are clearly observed, but the peak of H_2^+ is very small, the same as in Fig. 6. Therefore, the optimal B field for the generation of the hydrogen pair-ion plasma with high density is governed by the balance of the production efficiency of H^+, the electron removal by magnetic filtering, and the diffusion loss of the particles.

As already noted, the ion cyclotron frequency, depending on the ion species and the B field, is several MHz or less, while the electron cyclotron frequency is 10^3–10^4 times higher. In general, it is not easy to apply microwave power of the electron cyclotron frequency to the top plate with a wide area. Thus the cyclotron-resonance principle is not applicable to confirming the existence of electrons. For this purpose, the principle of dc $E\times B$ drift ($E\times B$ drift method) is adopted instead of the cyclotron-resonance principle. As already mentioned, the $E\times B$ drift collector grounded via a resistance is set at the center of the side plate of the omegatron, as shown in Fig. 4(b). Positive- or negative-charged particles are selectively introduced into the omegatron by applying dc voltage to the front electrode. The particles are accelerated in the sheath formed in front of the front electrode, and their velocity depends on their mass even if the acceleration voltage (the sheath depth) is the same. When a dc-E field is formed in the omegatron, the guiding center of the particles moves in the E×B direction with drift velocity E/B, which is independent of their charge and mass. Their orbit is determined by the sum of the parallel velocity and the perpendicular drift, thus the E field at which the charged particles can reach the $E\times B$ collector depends on the particle species. This method has no advantage over the cyclotron-resonance method in mass resolution, but it is effective for separation measurement in currents of electrons and negative ions with large mass difference. Here, since the plasma flows directly after its production in the PIG-discharge part in the absence of the negative-ion and ion-selection parts, the charged particles to be analyzed consist of H^+, H_2^+, H_3^+, and electrons that reach the omegatron.

The dc ion current I_{EB} of the $E\times B$ drift collector is measured as a function of the dc E field using a resistor of 1 MΩ, as shown in Fig. 8. Only positive ions enter into the omegatron at V_{fr}=−60 V. When a comparatively large E field ($E>20$ V/cm) is applied, the positive ions reach the collector. Positive peaks of I_{EB} at E ~47 V/cm and 70 V/cm are inferred to indicate the currents of H^+ and H_3^+, respectively. In contrast, when the front-electrode bias is increased to V_{fr}=0 V, electrons can enter and a sharp negative peak at E ~−1 V/cm is clearly observed, indicating the electron current. According to these results, the electron current and the positive-ion current can be measured separately. The H^- current with a negative peak is expected to be observed similarly to the H^+ current when negative ions are produced and only negative-charged particles enter into the omegatron. It is important to remove electrons completely in pair-ion plasma generation. In a pure pair-ion plasma without electrons, the negative current of the Langmuir probe consists of only the negative ions. When the pair plasma is not pure, a minute electron current overlaps the negative-ion current in the current-voltage characteristics determined by Langmuir probe measurement. However, the measurement technique proposed here enables us to trace the existence of electrons in the plasma, since the negative-ion current and the electron current can be measured separately as described above.

V. CONCLUSIONS

A fullerene pair-ion plasma, consisting of C_{60}^+ and C_{60}^- of equal mass without electrons, is generated using a hollow electron beam in a magnetic field, where electron-impact ionization and electron attachment play a key role. The active excitation of density modulation by a cylindrical exciter reveals the properties of electrostatic modes propagating along the magnetic-field lines: an ion acoustic wave dividing into two branches at around the ion cyclotron frequency, an ion plasma wave, and an intermediate-frequency wave. The phase lag between the density fluctuations of positive and negative ions for IAW strongly depends on the frequency, but the phase lags for IPW and IFW remain almost constant at a constant value of π.

The response frequency of the fullerene pair-ion plasma is limited to the narrow frequency range. The pair-ion plasma consisting of hydrogen ions ($H^+ - H^-$) with a small mass and high-frequency response to electromagnetic fields is attractive for investigating unique collective phenomena. As a first step, the positive ions H^+, H_2^+, and H_3^+ are produced in a PIG discharge. The ion species are analyzed using the omegatron of an rf mass spectrometer, and H^+ and H_3^+ are found to be dominant in the plasma. For the inspection of the existence of electrons in pair-ion plasmas, stationary $E \times B$ drift motion of the charged particles is utilized for the separation of the electron current and the ion currents, and a sharp electron current peak as a function of the dc-E field is separately observed.

ACKNOWLEDGMENTS

The authors would like to thank N. Tomioka, M. Musashi (Kobayashi), D. Date, H. Iwata, Y. Kuwabara, J. Terashima, and T. Kaneko for their collaboration.

This work was supported by a Grant-in-Aid for Scientific Research from the Ministry of Education, Culture, Sports, Science, and Technology, Japan.

[1] G. A. Stewart and E. W. Laing, J. Plasma Phys. **47**, 295 (1992).
[2] N. Iwamoto, Phys. Rev. E **47**, 604 (1993).
[3] J. Zhao, K. I. Nishikawa, J. I. Sakai, and T. Neubert, Phys. Plasmas **1**, 103 (1994).
[4] G. A. Stewart, J. Plasma Phys. **50**, 521 (1993).
[5] S. Y. Abdul-Rassak and E. W. Laing, J. Plasma Phys. **50**, 125 (1993).
[6] G. P. Zank and R. G. Greaves, Phys. Rev. E **51**, 6079 (1995).
[7] J. Zhao, J. I. Sakai, and K.-I. Nishikawa, Phys. Plasmas **3**, 844 (1996).
[8] C. M. Surko, M. Leventhal, and A. Passner, Phys. Rev. Lett. **62**, 901 (1989).
[9] C. M. Surko and T. J. Murphy, Phys. Fluids B **2**, 1372 (1990).
[10] M. D. Tinkle, R. G. Greaves, and C. M. Surko, Phys. Plasmas **2**, 2880 (1995).
[11] H. Boehmer, M. Adams, and N. Rynn, Phys. Plasmas **2**, 4369 (1995).
[12] R. G. Greaves and C. M. Surko, Phys. Plasmas **4**, 1528 (1997).
[13] E. P. Liang, S. C. Wilks, and M. Tabak, Phys. Rev. Lett. **81**, 4887 (1998).
[14] N. Sato, T. Mieno, T. Hirata, Y. Yagi, R. Hatakeyama, and S. Iizuka, Phys. Plasmas **1**, 3480 (1994).
[15] W. Oohara, S. Ishiguro, R. Hatakeyama, and N. Sato, J. Phys. Soc. Jpn. **71**, 373 (2002).
[16] W. Oohara, R. Hatakeyama, and S. Ishiguro, Plasma Phys. Controlled Fusion **44**, 1299 (2002).
[17] W. Oohara, R. Hatakeyama, and S. Ishiguro, Phys. Rev. E **68**, 066407 (2003).
[18] W. Oohara and R. Hatakeyama, Phys. Rev. Lett. **91**, 205005 (2003).
[19] R. Hatakeyama and W. Oohara, Phys. Scr. **T116**, 101 (2005).
[20] W. Oohara, Y. Kuwabara, and R. Hatakeyama, AIP Conf. Proc. **799**, 29 (2005).
[21] W. Oohara, D. Date, and R. Hatakeyama, Phys. Rev. Lett. **95**, 175003 (2005).
[22] R. Völpel, G. Hofmann, M. Steidl, M. Stenke, M. Schlapp, R. Trassl, and E. Salzborn, Phys. Rev. Lett. **71**, 3439 (1993).
[23] S. Matt, B. Dünser, M. Lezius, H. Deutsch, K. Becker, A. Stamatovic, P. Scheier, and T. D. Märk, J. Chem. Phys. **105**, 1880 (1996).
[24] T. Jaffke, E. Illenberger, M. Lezius, S. Matejcik, D. Smith, and T. D. Märk, Chem. Phys. Lett. **226**, 213 (1994).
[25] J. Haung, H. S. Carman, Jr., and R. N. Compton, J. Phys. Chem. **99**, 1719 (1995).
[26] D. P. Sheehan and N. Rynn, Rev. Sci. Instrum. **59**, 1369 (1988).
[27] P. K. Shukla, Phys. Scr. **T113**, 7 (2004).
[28] P. K. Shukla and M. Khan, Phys. Plasmas **12**, 014504 (2005).
[29] A. Hasegawa and P. K. Shukla, Phys. Scr. **T116**, 105 (2005).
[30] F. Verheest and T. Cattaert, Phys. Plasmas **12**, 032304 (2005).
[31] H. Schamel and A. Luque, New J. Phys. **7**, 69 (2005).
[32] P. K. Shukla and L. Stenflo, Phys. Plasmas **12**, 044503 (2005).
[33] B. Eliasson and P. K. Shukla, Phys. Rev. E **71**, 046402 (2005).
[34] F. Verheest and G. S. Lakhina, New J. Phys. **7**, 94 (2005).
[35] J. Vranjes and S. Poedts, Plasma Sources Sci. Technol. **14**, 485 (2005).
[36] F. Verheest, Nonlinear Processes Geophys. **12**, 569 (2005).
[37] A. Luque, H. Schamel, B. Eliasson, and P. K. Shukla, Phys. Plasmas **12**, 122307 (2005).
[38] H. Saleem, J. Vranjes, and S. Poedts, Phys. Lett. A **350**, 375 (2006).
[39] A. Luque, H. Schamel, B. Eliasson, and P. K. Shukla, Plasma Phys. Controlled Fusion **48**, L57 (2006).
[40] Z. Jian, Chin. Phys. **15**, 1028 (2006).
[41] H. Saleem, Phys. Plasmas **13**, 044502 (2006).
[42] I. Kourakis, A. Esfandyari-Kalejahi, M. Mehdipoor, and P. K. Shukla, Phys. Plasmas **13**, 052117 (2006).
[43] H. Sommer, H. A. Thomas, and J. A. Hipple, Phys. Rev. **82**, 697 (1951).
[44] B. M. Wilson and P. D. George, Rev. Sci. Instrum. **27**, 720 (1956).
[45] E. Y. Wang, L. Schmitz, Y. Ra, B. LaBombard, and R. W. Conn, Rev. Sci. Instrum. **61**, 2155 (1990).
[46] T. Hirata, R. Hatakeyama, Y. Yagi, T. Mieno, S. Iizuka, and N. Sato, J. Plasma Fusion Res. **71**, 615 (1995).
[47] T. Murakami, T. Kaneko, J. Terashima, R. Hatakeyama, S. Murase, and S. Shimamoto, J. Appl. Phys. **92**, 6423 (2002).
[48] A. V. Phelps, J. Phys. Chem. Ref. Data **19**, 653 (1990).
[49] D. A. Church, Phys. Rep. **228**, 253 (1993).
[50] H. Higaki, N. Kuroda, K. Yoshiki Franzen, Z. Wang, M. Hori, A. Mohri, K. Komaki, and Y. Yamazaki, Phys. Rev. E **70**, 026501 (2004).